RSC Advances

ROYAL SOCIETY OF CHEMISTRY

www.rsc.org/advances

A label-free amperometric immunosensor for the detection of carcinoembryonic antigen based on novel magnetic carbon and gold nano composites

Faying Li[1], Liping Jiang[1], Jian Han[1], Qing Liu[1], Yunhui Dong[1], Yueyun Li[1]*, Qin Wei[2]

1. School of Chemical Engineering, Shandong University of Technology, Zibo, 255049, P.R. China

2. Key Laboratory of Chemical Sensing & Analysis in Universities of Shandong, School of Chemistry and Chemical Engineering, University of Jinan, Jinan, 250022, P.R. China

*: Corresponding author:

Email address: liyueyun71@163.com

Fax: +86-533-2781664

Tel: +86-533-2781225

ABSTRACT

In this work, a novel label-free electrochemical immunosensor was developed for the quantitative detection of carcinoembryonic antigen (CEA). To this end, gold nanoparticles (Au NPs) functionalized magnetic multi-walled carbon nanotubes (MWCNTs-Fe_3O_4) were prepared and applied for lead ions (Pb^{2+}) adsorption. Because the synergetic effect presents in Pb^{2+}@Au@MWCNTs-Fe_3O_4, it shows better electrocatalytic activity towards the reduction of hydrogen peroxide (H_2O_2) than MWCNTs, MWCNTs-Fe_3O_4 or Au@MWCNTs-Fe_3O_4. Featured by large specific surface area, good biocompatibility and excellent electrical conductivity, Pb^{2+}@Au@MWCNTs-Fe_3O_4 was used as transducing materials to achieve efficient conjugation of capture antibodies and signal amplification of the proposed immunosensor. Cyclic voltammetry and amperometric i-t technique were used to record the change of electrochemical signal when the electrodes were modified with different concentrations of CEA. Under the optimal conditions, the label-free immunosensor exhibited a wide linear range from 5 fg/mL to 50 ng/mL with a low detection limit of 1.7 fg/mL for CEA. The proposed immunosensor displays high electrochemical performance with good reproducibility, selectivity and stability, which has great potential in clinical and diagnostic applications.

Keywords: Label-free immunosensor; Carcinoembryonic antigen;

Multi-walled carbon nanotubes; Gold nanoparticles; Lead ions.

1. Introduction

Cancer has been regarded as one of the major causes of mortality worldwide and its effective treatment still has not been reported [1]. In clinical analysis, the cancer patients can be detected when the concentration of tumor markers is enhanced to a certain level in serum[2]. Hence, it is quite necessary to achieve sensitive, fast, and accurate assays for the monitor of tumor markers for effective early diagnosis and therapeutics of cancer [1, 3, 4]. Carcinoembryonic antigen (CEA) is a member of a family of cell surface glycoproteins, which are produced in excess in essentially all human colon carcinomas and in a high proportion of carcinomas at many other sites [5, 6]. As a widely used tumor maker of human colon carcinomas, the quantitative detection of CEA in serum is valuable in diagnosis or clinical manage [6].

In the past few years, a variety of methods have been applied to detect tumor markers, such as electrochemical immunosensors [7, 8], enzyme-linked immunosorbent assay [9, 10], ECL immunosensor [11], **e**lectrochemiluminescence immunoassay [11-14]. For comparisons, electrochemical immunosensors have attracted widespread attention due to their high sensitivity, rapid, highly selective and simple operation [15, 16]. Among all of the electrochemical immunosensors, label-free electrochemical immunosensors have recently emerged as a novel assay to detect proteins due to their simple preparation, more cost effectiveness

and well activity conservation of antibodies or antigens [15, 17].

In order to improve the sensitivity of electrochemical analysis, a variety of nanomaterials have been used to fabricate immunosensors to achieve signal amplification, such as carbon nanotubes [18, 19], metal nanoparticles [20-22],and metal oxides [23]. Among these tested materials, multi-walled carbon nanotubes (MWCNTs) get the most attention due to their large specific surface area, excellent conductivity [24, 25] and good biocompatibility [26, 27]. Fe_3O_4 has a great auxiliary catalytic activity towards the reduction of hydrogen peroxide (H_2O_2) according to previous reports [28]. Simultaneously, Fe_3O_4 nanoparticles can promote the electron transfer, thus providing a better choice to fabricate electrochemical immunosensors [15]. Metal NPs dispersed on an oxide support often display higher catalytic activity than these NPs as a single component, which is due to the synergetic effect occurring at the interface between metal and oxide support [28-30]. Recent studies declared that Au NPs deposited on a metal-oxide support showed high catalytic activity for CO oxidation even though Au NPs are chemically inert [28]. The surface functionalization of MWCNTs would provide an avenue for further chemical modification, such as ion adsorption [31, 32]. As a kind of protein containing amino groups ($–NH_2$), primary antibodies (Ab_1) can be effectively conjugated onto the Au@MWCNTs-Fe_3O_4 by the interaction between Au NPs and $–NH_2$ on antibodies to construct Au–N [6, 33, 34].

Au@MWCNTs-Fe_3O_4 has a large surface area, high conductivity and exceptional adsorption capability for lead ions (Pb^{2+}) due to the synergetic effect, which is applied to signal amplification. After adsorbing Pb^{2+}, the redox process of Pb^{2+} could further promote the redox process of H_2O_2, which was applied to signal amplification. The signal amplification strategy, using the synergetic effect present in gold nanoparticles functionalized magnetic multi-walled carbon nanotubes loaded with lead ions (Pb^{2+}@Au@MWCNTs-Fe_3O_4), can further increase electron transfer efficiency on electrode surface and the reaction efficiency of the nanocomposite toward H_2O_2 reduction to improve the detection sensitivity of the immunosensor [15, 28].

In this research, an innovative label-free electrochemical immunosensor was designed to achieve quantitative detection of CEA. The synergetic effect existing in the Pb^{2+}@Au@MWCNTs-Fe_3O_4 system, it could not only improve the electron transfer efficiency but also enhance the effective immobilization of Ab_1. The proposed immunosensor provides a useful technology for the quantitative detection of CEA in human serum, which shows the advantages of wide linear range, low detection limit, good reproducibility and selectivity, as well as acceptable stability. The results of electrochemical studies suggested that the proposed immunosensor possessed great performance for CEA determination and provided a great potential application for the analysis

of other low-abundant proteins.

2. Material and methods

2.1. Apparatus and reagents

CHI760D electrochemical workstation was used in the entire process of electrochemical measurement (Shanghai CH Instruments Co, China). Scanning electron microscope (SEM) images were obtained using Quanta FEG250 field emission environmental SEM (FEI, United States). Energy Dispersive X-Ray spectra (EDX) were recorded by JEOL JSM-6700F microscope (Japan). For A.C. impedance measurements, a frequency range of 0.1 kHz to 100 Hz and AC voltage amplitude of 5 mV were used.

CEA antibody and antigen were purchased from Beijing Dingguochangsheng Biotechnology Co. Ltd. China. Bovine serum albumin (BSA, 96-99%) was purchased from Sigma reagent co., Ltd. (St. Louis, MO, USA). Multi-walled carbon nanotubes (MWCNTs) were purchased from Alfa Aesar co., Ltd. (Shanghai, China). $HAuCl_4 \cdot 4H_2O$ were obtained from Sinopharm Chemical Reagent Shanghai Co.,Ltd., China. $FeCl_3 \cdot 6H_2O$ was purchased from Damao Chemical Reagent Tianjin Co., Ltd., China. $K_3Fe(CN)_6$ was purchased from Sinopharm Chemical Reagent Co., Ltd. (Beijing, China). Phosphate buffered saline (PBS, pH=7.4) were prepared as an electrolyte in the electrochemical measurement. The Ab_1 solution was prepared as follows: 1mg of CEA

antibody was dissolved in PBS (pH=7.4, 10mL) to obtain Ab_1 stock solutions. Subsequently, it was diluted to the required concentration (10 μg/mL). Ultrapure water (18.25 MΩ cm, 24 °C) was used throughout the study. All other reagents are at analytical grade. All solutions were stored at 4 °C for frequent usage.

2.2. Preparation of the amino-functionalized MWCNTs-Fe_3O_4

To remove all the metal oxide, MWCNTs (0.5 g) was added into a mixture of 3M HNO_3 and 2M H_2SO_4 (3:1, v/v), which was kept under ultrasonic conditions at 40 °C for 3 h before cooled down to room temperature. Then it was washed to neutrality, and dried at room temperature.

MWCNTs-Fe_3O_4 was synthesized according to an established protocol [35]. In brief, $FeCl_3 \cdot 6H_2O$ (0.7 g) and MWCNTs (0.2 g) were dissolved in ethylene glycol (37.5 mL) to form a clear solution. Subsequently, sodium acetate (NaAc, 1.8 g) was added and dissolved under ultrasonic conditions. The mixture was stirred vigorously for 30 min and then transferred to a teflon-lined stainless steel autoclave. The autoclave was heated to 200 °C and maintained at this temperature for 16 h, and finally cooled down to room temperature. Ultra-pure water (50 mL) was used to clean the composite and the resultant was separated from the liquid mixture using a strong magnet.

MWCNTs-Fe_3O_4 (0.1 g) and 3-aminopropyl triethoxysilane (0.1mL)

were dissolved in anhydrous ethanol (10 mL) and heated to 70 °C for 1.5 h. Subsequently, it was separated by magnetic separation and washed by anhydrous ethanol. Then the desired amino-functionalized MWCNTs-Fe_3O_4 was stored at 50 °C.

2.3 Preparation of Au@MWCNTs-Fe_3O_4

The preparation of Au NPs was according to the reduction of $AuCl_4^-$ ions by the sodium citrate [36]. In brief, Sodium citrate (1.5 mL, 10 mg/mL) was added to the aqueous solution (100 mL) containing $HAuCl_4$ (1 wt%, 1 mL). Then, the mixture was heated to reflux and kept for 15 min. After cooled down, the mixture was stored at 4 °C, which provided an Au NPs solution in wine red.

Then the prepared amino-functionalized MWCNTs-Fe_3O_4 (10 mg) was added to the Au NPs (20 mL) solution. The suspension was stirred for 12 h. Au NPs could bind with all of amino groups on the surface of amino-functionalized MWCNTs- Fe_3O_4. The sediment was dried and the obtained powder was designated as Au@MWCNTs-Fe_3O_4.

2.4 Preparation of Pb^{2+}@Au@MWCNTs-Fe_3O_4

Au@MWCNTs-Fe_3O_4 (4 mg) was dispersed into lead nitrate solution (4mL, 1mg/mL). The solution was oscillated for 24 hours to achieve the goal that Pb^{2+} was absorbed as much as possible onto the Au@MWCNTs-Fe_3O_4. The Pb^{2+}@Au@MWCNTs-Fe_3O_4 was obtained for further use after magnetic separation. The

Pb^{2+}@Au@MWCNTs-Fe_3O_4 solution was prepared as follows: a certain amount of Pb^{2+}@Au@MWCNTs-Fe_3O_4 was dispersed in ultrapure water to obtain the required concentration. Fig. 1A shows the preparation procedure of Pb^{2+}@Au@MWCNTs-Fe_3O_4.

2.5 Fabrication of the immunosensor

Fig. 1B shows the fabrication process of the label-free electrochemical immunosensor. A bare glassy carbon electrode (GCE) was polished repeatedly by using alumina powder and thoroughly washed. The pretreated bare glassy carbon electrode (GCE) was coated with Pb^{2+}@Au@MWCNTs-Fe_3O_4 (2 mg/mL, 6mL) and dried under atmospheric temperature. Following that, the resultant electrode was incubated with Ab_1 (10 μg/mL, 6 μL) and dried at 4 °C. After storing at 4 °C for drying, the nonspecific binding sites for CEA were blocked by 3 μL of 1 wt% bovine serum albumin (BSA) at room temperature for 1 h. Subsequently, the electrode was washed thoroughly with PBS (pH=7.4). The fabricated immunosensor could recognize different concentrations of CEA (5 fg/mL to 50 ng/mL, 6 mL) based on immunoreaction at room temperature for 1 h. The proposed immunosensor was stored at 4 °C for further usage.

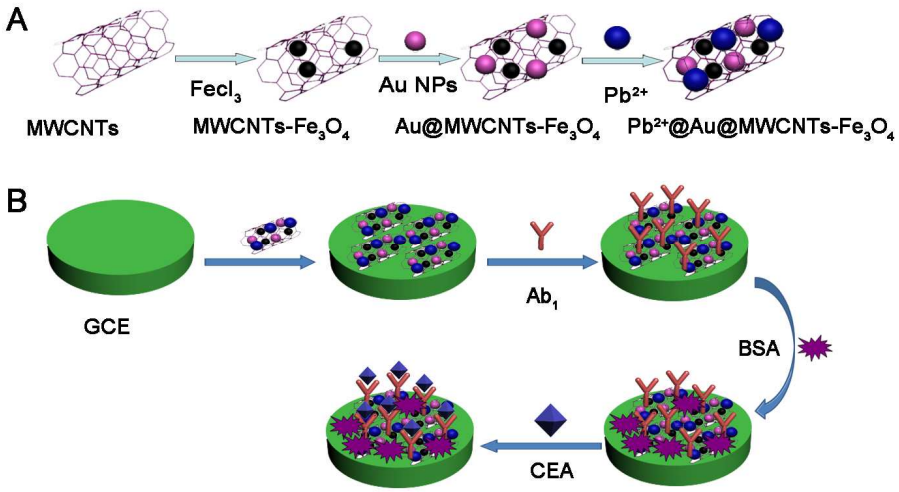

Fig.1. (A) The preparation procedure of Pb^{2+}@Au@MWCNTs-Fe_3O_4; (B) The fabrication process of the label-free electrochemical immunosensor.

2.6 Detection of CEA

All electrochemical measurements were carried out with a conventional three-electrode system using a GCE (4 mm in diameter) as a working electrode, a platinum wire as a counter electrode and a saturated calomel electrode (SCE) as a reference electrode. The PBS at pH=7.4 was used for all the electrochemical measurements. All cyclic voltammetry experiments (CVs) were performed in the conventional electrochemical cell by scanning the potential from -1.0 V to 1.0 V. Amperometric i–t curve was used to record the amperometric responses at -0.4 V. After the current stability under stirring, 5 mM H_2O_2 was added into the PBS and the current change was recorded.

3. Results and discussion

3.1 Morphology of MWCNTs-Fe_3O_4 and Au@MWCNTs-Fe_3O_4

composites

As can be seen from the SEM image (Fig.2A), the untreated carbon nanotubes shows thin long tubular shape and were irregularly agglomerated. After magnetization, there were a lot of nearly monodispersed microspheres around 120 nm uniformly attached on the surface of MWCNTs which proving the morphology change before and after Fe_3O_4 loading (Fig.2B). EDX spectra (Fig. 2D) confirms the presence of Fe_3O_4 in the sample after magnetization. This also proved that the magnetic field presents significant effect on the dispersion (Fig 2F). Furthermore, FTIR spectroscopy was used to verify each step of the MWCNTs functionalization. As shown in Fig 2G, the peak at 3420 cm^{-1} corresponding to the hydroxyl group stretching vibration, two peaks at 1631 and 1050 cm^{-1} corresponded to the carboxyl[37] and carbonyl[8] stretching vibrations. The absorption at 1431 cm^{-1} was due to the COO–Fe bond[38]. A peak (spectrum b) at 573 cm^{-1} was typical Fe–O stretching vibration[39] of the prepared MWCNT@Fe_3O_4 composites. All of these are evidence for the synthesized material. When the Au NPs were loaded onto the MWCNTs-Fe_3O_4, the surface morphology was greatly altered. Many light particles around 20 nm were loaded on the MWCNTs-Fe_3O_4 by Au NPs and $–NH_2$ on the surface of amino-functionalized MWCNTs- Fe_3O_4 to construct Au–N (Fig. 2C). The EDX analysis of the Au@MWCNTs-Fe_3O_4 sample confirms the presence

of C, Fe, Au and O elements (Fig. 2E).

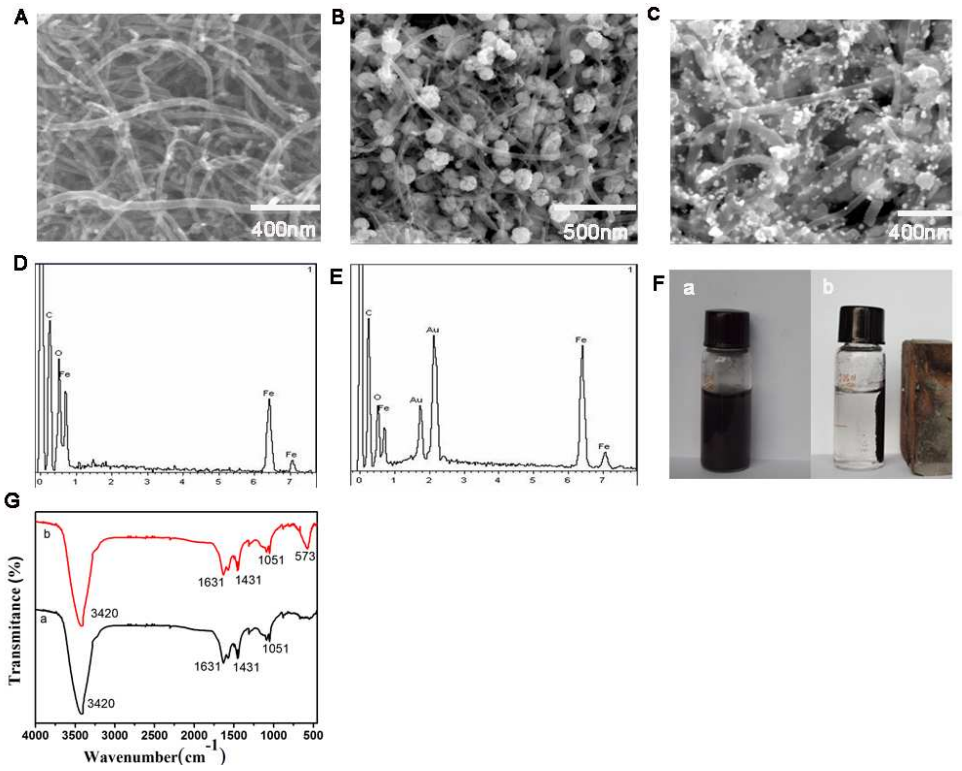

Fig.2. The SEM image of MWCNTs (A); MWCNTs-Fe_3O_4 (B); Au@MWCNTs-Fe_3O_4 (C); EDX spectrum of the MWCNTs-Fe_3O_4 (D); EDX spectrum of the Au@ MWCNTs-Fe_3O_4 (E); Comparison of MWCNTs-Fe_3O_4 solution in the absence (a) and presence (b) of a magnet (F).

3.2. Comparison of the electron transfer ability of different materials

For label-free immunosensors, the sensitivity is very dependent on the transducing material. In order to verify that Pb^{2+}@Au@MWCNTs-Fe_3O_4 possess superior electrochemical performance, Au NPs, MWCNTs, MWCNTs-Fe_3O_4, Au@MWCNTs-Fe_3O_4 and Pb^{2+}@Au@MWCNTs-Fe_3O_4 were loaded onto the GCE surface

respectively for electrocatalytic performance of H_2O_2 reduction (Fig. 3A). Tested by amperometric i-t curve, a weak signal was detected when Au NPs (curve a) and MWCNTs (curve b) were loaded onto the electrode respectively. Fe_3O_4 has a great auxiliary catalytic activity towards H_2O_2 reduction essentially [28]. When MWCNTs-Fe_3O_4 was used to modify the bare GCE, a much larger current response was observed (curve c). The electrochemical signal was further increased (curve d) when Au@MWCNTs-Fe_3O_4 was loaded onto the electrode. As expected, the immunosensor using Pb^{2+}@Au@ MWCNTs-Fe_3O_4 to modify bare GCE displayed the highest current change (curve e). These results suggest that Pb^{2+} and Au NPs promote the multiple signal amplification toward the reduction of H_2O_2 as an analytical signal. The Pb^{2+}@Au@MWCNTs-Fe_3O_4 possesses excellent electrochemical performance to improve the sensitivity of the proposed immunosensor.

CV was used to further prove the successful adsorption of Pb^{2+} in Fig.3 B. It could be found that an oxidation peak potential around −0.25 V when a bare GCE was scanned in a 0.1 mg/mL of Pb^{2+} solution (curve a). The oxidation peak was also found around −0.25 V when the electrode was scanned (curve b) in PBS (pH=7.4) using Pb^{2+}@Au@MWCNTs-Fe_3O_4 as the transducing material. From the comparison, it was obvious that Pb^{2+} was adsorbed successfully. Subsequently, the immunosensor using Pb^{2+}@Au@MWCNTs-Fe_3O_4 as

the transducing material was scanned in PBS (pH=7.4) with the addition of 5 mM H_2O_2. After the addition of H_2O_2, a dramatic increase of the reduction current (curve c) was observed at the same potential, which indicates the Pb^{2+}@Au@MWCNTs-Fe_3O_4 has a good electrocatalytic performance towards the reduction of H_2O_2.

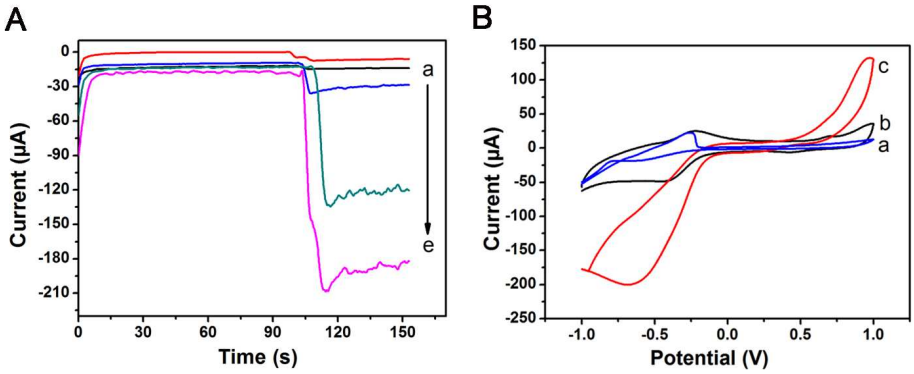

Fig.3. (A) Ameperometic response of the immunosensors with different materials: (a) Au NPs, (b) MWCNTs, (c) MWCNTs-Fe_3O_4, (d) Au@MWCNTs-Fe_3O_4, (e) Pb^{2+}@Au@MWCNTs- Fe_3O_4; (B) CV of the immunosensor using Pb^{2+}@Au@MWCNTs-Fe_3O_4 as transducing material in PBS at pH=7.4 before (curve b) and after (curve c) the addition of 5 mM H_2O_2. For comparison purposes, a bare GCE was scanned in 0.1 mg/mL of Pb^{2+} from -1.0V to 1.0 V (curve a).

3.3. Optimization of experimental conditions

In order to obtain better electrochemical signal, experimental conditions including pH and the concentration of Pb^{2+}@Au@MWCNTs-Fe_3O_4 were optimized. Firstly, the pH of the PBS

has a great influence on the electrochemical properties of the immunosensors. As shown in Fig.4A, the current signal increases with the variation of pH from 5.6 to 7.4, and then decreases with the variation of pH from 7.4 to 8.7. The pH value of 7.4 presents the largest electrochemical signal. The experimental results show that the optimal current signal was achieved at pH 7.4. Therefore, PBS at pH 7.4 was used as an electrolyte for electrochemical tests.

The concentration of the Pb^{2+}@Au@MWCNTs-Fe_3O_4 which was loaded on the surface of the electrode has important implications to the response of the electrochemical sensor. Amperometric i-t method was used to investigate the electrochemical signal response of different concentrations of Pb^{2+}@Au@MWCNTs-Fe_3O_4. As seen in Fig.4B, with the increase of the concentration from 0.5 mg/mL to 2.0 mg/mL, the current responses first increased, and then decreased with a further concentration increase from 2.0 to 3.5 mg/mL. The increase of Pb^{2+}@Au@MWCNTs-Fe_3O_4 film thickness may lead to an increase of interface electron transfer resistance. Therefore, the concentration of 2.0 mg/mL was used as the optimal concentration in this study.

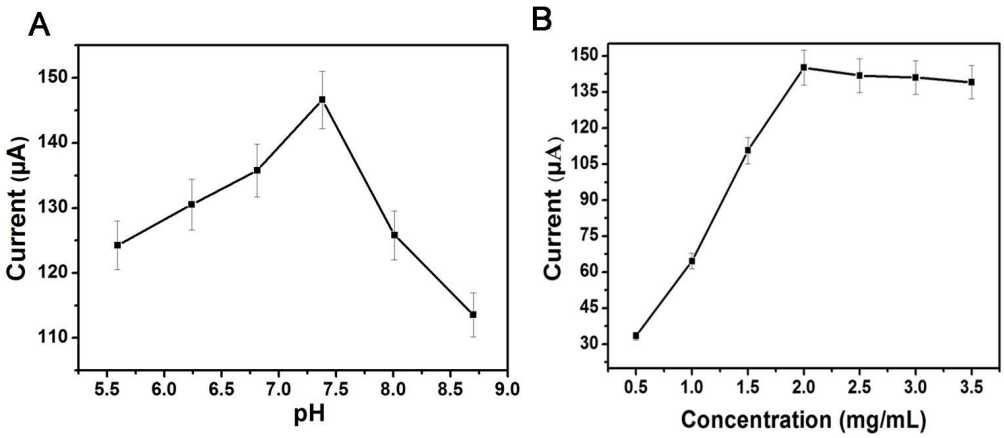

Fig.4. The optimization of experimental conditions with pH (A), Pb^{2+}@Au@MWCNTs-Fe_3O_4 concentration (B), Error bar=RSD (n=5).

3.4. Characterization of the immunosensor

Electrochemical impedance spectroscopy (EIS) is regarded as an effective method to probe the process of a modified electrode surface [40, 41]. A typical impedance spectrum includes a semicircle portion and a straight line portion. The semicircle portion represents the electron-transfer-limited process which can be observed at higher region. The linear portion represents the diffusion-limited process at lower frequencies. The semicircle diameter equals the electron-transfer resistance [41].

The Nyquist plots of electrochemical impedance spectroscopy were recorded from 0.1 to 10^5 Hz at 0.24 V in a solution containing 0.1 M KCl and 2.5 mmol/L Fe $(CN)_6^{3-}$/$Fe(CN)_6^{4-}$. As shown in Fig. 5A, bare GCE exhibited a very small semicircle diameter (curve a), suggesting a diffusional limiting step of the electrochemical process. It can be seen

that the semicircle is much smaller (curve b) than that of bare GCE when Pb^{2+}@Au@MWCNTs-Fe_3O_4 was loaded on the surface of the GCE. The reason for this observation was that Pb^{2+}@Au@MWCNTs-Fe_3O_4 is an excellent electrically conducting material, which could accelerate the electron transfer and make electron transfer easier. Then, after incubation with Ab_1, the resistance was significantly increased, demonstrating that Ab_1 was immobilized on the electrode successfully and blocked the electron transfer between the base solution and electrode (curve c). Similarly, when the BSA was loaded onto the electrode surface, the resistance was significantly increased (curve d). Another possible reason is that the modified protein molecules on the surface of the electrode greatly block the transfer of electrons. Additionally, resistance further increased with the addition of CEA (curve e), because the additions resist the electron-transfer kinetics of the redox probe at the electrode interface. As a result, we can conclude that the biosensor has been fabricated successfully.

Under the optimal conditions, a label-free electrochemical immunosensor using Pb^{2+}@Au@MWCNTs-Fe_3O_4 as transducing material was applied to detect different concentrations of CEA by amperometric i-t curve in pH 7.4 PBS at −0.4 V. The relationship between the amperometric response towards the reduction of H_2O_2 and CEA concentration is shown in Fig. 5B. As can be seen (Fig 5C), a linear

relationship between the amperometric response and the logarithmic values of CEA concentration was observed within the range of 0.005 pg/mL ~ 50 ng/mL with a detection limit of 1.7 fg/mL. The regression equation of the calibration curve is: I = -2.714 log (C/5) + 4.219, with correlation coefficient of 0.9960 at a signal to noise ratio (S/N) of 3. The low detection limit might be attributed to that Pb^{2+}@Au@MWCNTs-Fe_3O_4 conjugated to amounts of capture antibodies and the synergetic effect presented in Pb^{2+}@Au@MWCNTs-Fe_3O_4 that favor electron transfer. They could greatly increase the response to H_2O_2, broaden the scope of testing and lead to higher sensitivity.

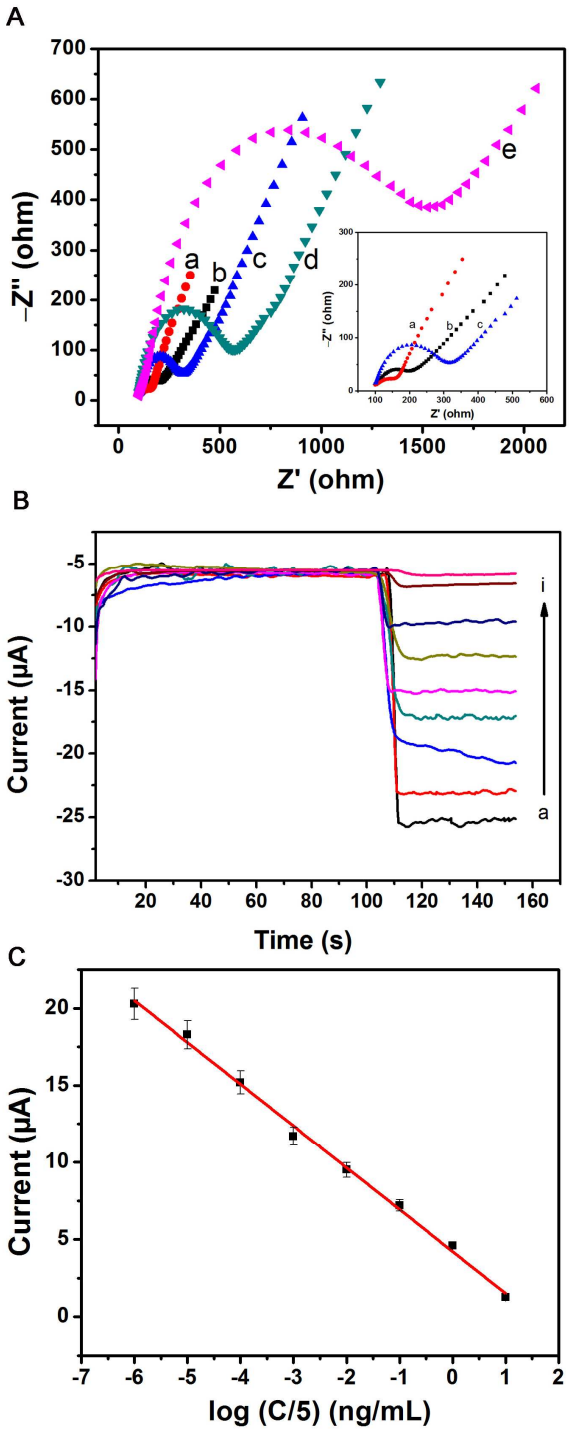

Fig. 5. (A) Nyquist plots of the AC impedance for each immobilized step recorded from 1 to 10^5 Hz of bare GCE (a), Pb^{2+}@Au@MWCNTs -Fe_3O_4/GCE (b), Pb^{2+}@Au@MWCNTs-Fe_3O_4 @Ab_1/GCE (c), BSA/Pb^{2+}@Au@MWCNTs-Fe_3O_4@Ab_1/GCE (d), CEA/BSA/ Pb^{2+}@Au

@MWCNTs-Fe_3O_4 @Ab_1/GCE (e) in PBS at pH=7.4 containing 0.1 M KCl and 2.5 mM $Fe(CN)_6^{3-}$/$Fe(CN)_6^{4-}$; (B) Amperometric response of the immunosensor for the varied concentration of CEA at -0.4 V (5 mM H_2O_2): (a) 5 fg/mL, (b) 50 fg/mL, (c) 500 fg/mL, (d) 5 pg/mL, (e) 50 pg/mL, (f) 500 pg/mL, (g) 5 ng/mL, (h) 50 ng/mL, (i) 100 ng/mL; (C) Calibration curve of the immunosensor toward different concentrations of CEA. Error bar=RSD (n=5).

3.5. Comparison of different methods

Compared with previously reported methods for the detection of CEA, this specially designed label-free immunosensor has a wider linear range and lower detection limit, as is shown in Table S1. In this work, Pb^{2+}@Au@ MWCNTs-Fe_3O_4 could not only immobilize the antibodies but also produce electrochemical signals. Consequently, high sensitivity is one of the advantages of this designed immunosensor.

3.6. Reproducibility, selectivity, and stability of the immunosensor

To evaluate the reproducibility of the immunosensor, five electrodes were prepared for the detection of 5 ng/mL of CEA. Amperometric i-t curve was used to record the electrochemical signal in PBS at pH 7.4 and the concentration of Pb^{2+}@Au@MWCNTs-Fe_3O_4 is 2.0 mg/mL. The relative standard deviation (RSD) of the measurements for the five

electrodes was 3.4% (Fig. 6A). The results suggested acceptable reproducibility and precision of the proposed immunoassay.

To investigate the selectivity of the proposed immunosensor, interference studies were performed using human IgG (HIgG), vitamin C, glucose and BSA. The 0.5 ng/mL of CEA solutions containing 50 ng/mL of interfering substances were measured by the proposed immunosensor and the results are shown in Fig. 6B. The result showed that the current variation due to the interfering substances was 4.4%, indicating the selectivity of the immunosensor was acceptable.

Stability of the immunosensors is also an important factor in their applications. The stability of the immunosensor was investigated by checking their current responses periodically. The immunosensor was stored in pH 7.4 PBS at 4 °C when not in use. It could be found that current responses to same concentration of CEA has no apparent change compared to the immunosensor freshly prepared which was used to directly detect the same concentration of CEA without being stored, suggesting the stability of the immunosensors was also acceptable. The reproducibility, selectivity and stability of this immunosensor were acceptable, thus suitable for the determination of CEA in real samples.

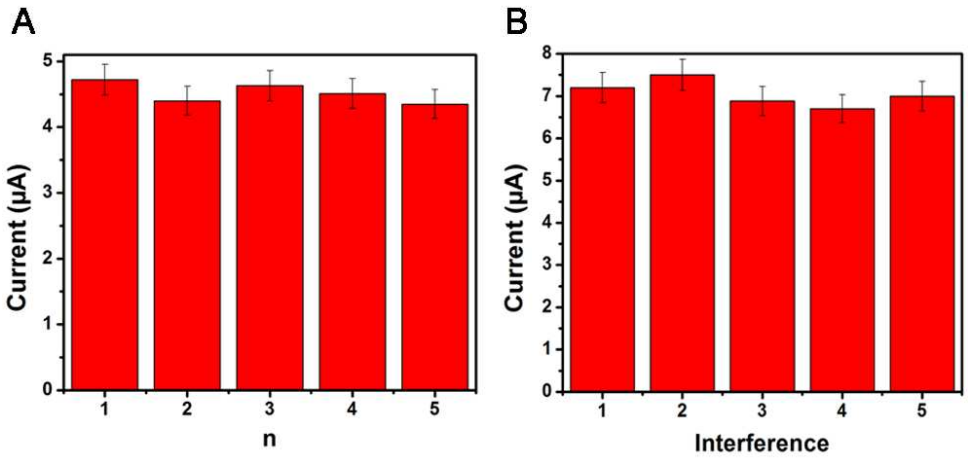

Fig. 6. (A) Amperometric change response of biosensor to different electrodes treated in same way; (B) Current responses of the immunosensor to 0.5 ng/mL CEA (1), 0.5 ng/mL CEA +50 ng/mL Human IgG (2), 0.5 ng/mL CEA +50 ng/mL vitamin C (3), 0.5 ng/mL CEA AFP +100 ng/mL glucose (4), 0.5 ng/mL CEA +100 ng/mL BSA (5). Error bar = RSD (n = 5).

3.7. Application of the immunosensor in serum sample

In order to evaluate the feasibility of the proposed immunosensor, it was applied to detect the recoveries of different concentrations of CEA in human serum samples by standard addition methods. As shown in Table S2, the recovery of CEA was from 97.5 % to 102.2 % and the relative standard deviation (RSD) was in the range from 3.90 % to 4.38%. The fact shows that the proposed immunoassay methodology could be clinically applied to the detection of the CEA concentrations in serum samples.

4. Conclusions

A novel electrochemical immunosensor for sensitive detection of CEA has been developed based on Pb^{2+}@Au@MWCNTs-Fe_3O_4 as signal amplifier. To ensure a high-performance electrochemical immunosensor, Pb^{2+}@Au@MWCNTs-Fe_3O_4 was immobilized on the electrode, which can increase the surface area to capture a larger amount of Ab as well as improve the electronic transmission rate. The proposed immunosensor has a linear response to the increased concentration of CEA from 5 fg/mL to 50 ng/mL. The proposed immunosensor is also characterized bya low detection limit, good reproducibility, excellent selectivity and stability. This proposed strategy might have a promising application in clinical immunoassay for other biomolecules.

Acknowledgments

This study was supported by the National Natural Science Foundation of China (Nos. 21375047, 21377046，21405095), the Project of Shandong Province Higher Educational Science and Technology Program (No. J14LC09)，and QW thanks the Special Foundation for Taishan Scholar Professorship of Shandong Province and UJN (No. ts20130937). All of the authors express their deep thanks.

References

[1] Jiang W, Yuan R, Chai Y, Mao L and Su H. A novel electrochemical immunoassay based on diazotization-coupled functionalized bioconjugates as trace labels for ultrasensitive detection of carcinoembryonic antigen[J]. *Biosensors and Bioelectronics*, 2011, 26(5): 2786-2790.

[2] Goldman R, Ressom H W, Varghese R S, Goldman L, Bascug G, Loffredo C A, Abdel-Hamid M, Gouda I, Ezzat S and Kyselova Z. Detection of hepatocellular carcinoma using glycomic analysis[J]. *Clinical Cancer Research*, 2009, 15(5): 1808-1813.

[3] Ferrari M. Cancer nanotechnology: opportunities and challenges[J]. *Nature Reviews Cancer*, 2005, 5(3): 161-171.

[4] Wulfkuhle J D, Liotta L A and Petricoin E F. Proteomic applications for the early detection of cancer[J]. *Nature Reviews Cancer*, 2003, 3(4): 267-275.

[5] Benchimol S, Fuks A, Jothy S, Beauchemin N, Shirota K and Stanners C P. Carcinoembryonic antigen, a human tumor marker, functions as an intercellular adhesion molecule[J]. *Cell*, 1989, 57(2): 327-334.

[6] Wang Y, Li X, Cao W, Li Y, Li H, Du B and Wei Q. Ultrasensitive sandwich-type electrochemical immunosensor based on a novel signal amplification strategy using highly loaded toluidine blue/gold nanoparticles decorated KIT-6/carboxymethyl chitosan/ionic liquids as

signal labels[J]. *Biosensors and Bioelectronics*, 2014, 61: 618-624.

[7] Liu S, Lin Q, Zhang X, He X, Xing X, Lian W and Huang J. Electrochemical immunosensor for salbutamol detection based on CS-Fe_3O_4-PAMAM-GNPs nanocomposites and HRP-MWCNTs-Ab bioconjugates for signal amplification[J]. *Sensors and Actuators B: Chemical*, 2011, 156(1): 71-78.

[8] Zarei H, Ghourchian H, Eskandari K and Zeinali M. Magnetic nanocomposite of anti-human IgG/COOH–multiwalled carbon nanotubes/Fe3O4 as a platform for electrochemical immunoassay[J]. *Analytical Biochemistry*, 2012, 421(2): 446-453.

[9] Zhang S, Yang J and Lin J. 3, 3′–diaminobenzidine (DAB)–H_2O_2–HRP voltammetric enzyme-linked immunoassay for the detection of carcionembryonic antigen[J]. *Bioelectrochemistry*, 2008, 72(1): 47-52.

[10] Yuan R, Zhuo Y, Chai Y, Zhang Y and Sun A. Determination of carcinoembryonic antigen using a novel amperometric enzyme-electrode based on layer-by-layer assembly of gold nanoparticles and thionine[J]. *Science in China Series B: Chemistry*, 2007, 50(1): 97-104.

[11] Wu B, Hu C, Hu X, Cao H, Huang C, Shen H and Jia N. Sensitive ECL immunosensor for detection of retinol-binding protein based on double-assisted signal amplification strategy of multiwalled carbon nanotubes and $Ru(bpy)_3^{2+}$ doped mesoporous silica nanospheres[J].

Biosensors and Bioelectronics, 2013, 50(0): 300-304.

[12] Zhuo Y, Gui G, Chai Y, Liao N, Xiao K and Yuan R. Sandwich-format electrochemiluminescence assays for tumor marker based on PAMAM dendrimer-l-cysteine-hollow gold nanosphere nanocomposites[J]. *Biosensors and Bioelectronics*, 2014, 53(0): 459-464.

[13] Feng X, Gan N, Zhou J, Li T, Cao Y, Hu F, Yu H and Jiang Q. A novel dual-template molecularly imprinted electrochemiluminescence immunosensor array using $Ru(bpy)_3^{2+}$-Silica@Poly-L-lysine-Au composite nanoparticles as labels for near-simultaneous detection of tumor markers[J]. *Electrochimica Acta*, 2014, 139(0): 127-136.

[14] Wang S, Zhang Y, Yu J, Song X, Ge S and Yan M. Application of indium tin oxide device in gold-coated magnetic iron solid support enhanced electrochemiluminescent immunosensor for determination of carcinoma embryonic antigen[J]. *Sensors and Actuators B: Chemical*, 2012, 171–172(0): 891-898.

[15] Yu S, Wei Q, Du B, Wu D, Li H, Yan L, Ma H and Zhang Y. Label-free immunosensor for the detection of kanamycin using $Ag@Fe_3O_4$ nanoparticles and thionine mixed graphene sheet[J]. *Biosensors and Bioelectronics*, 2013, 48(0): 224-229.

[16] He P, Wang Z, Zhang L and Yang W. Development of a label-free electrochemical immunosensor based on carbon nanotube for rapid determination of clenbuterol[J]. *Food Chemistry*, 2009, 112(3): 707-714.

[17] Marchesini G, Buijs J, Haasnoot W, Hooijerink D, Jansson O and Nielen M. Nanoscale affinity chip interface for coupling inhibition SPR immunosensor screening with nano-LC TOF MS[J]. *Analytical chemistry*, 2008, 80(4): 1159-1168.

[18] Zhang J, Lei J, Xu C, Ding L and Ju H. Carbon nanohorn sensitized electrochemical immunosensor for rapid detection of microcystin-LR[J]. *Analytical chemistry*, 2010, 82(3): 1117-1122.

[19] Kavosi B, Salimi A, Hallaj R and Amani K. A highly sensitive prostate-specific antigen immunosensor based on gold nanoparticles/PAMAM dendrimer loaded on MWCNTS/chitosan/ionic liquid nanocomposite[J]. *Biosensors and Bioelectronics*, 2014, 52(0): 20-28.

[20] Lan M, Chen C, Zhou Q, Teng Y, Zhao H and Niu X. Voltammetric detection of microcystis genus specific-sequence with disposable screen-printed electrode modified with gold nanoparticles[J]. *Advanced Materials Letters*, 2010, 1(3).

[21] Wang H, Wu J, Li J, Ding Y, Shen G and Yu R. Nanogold particle-enhanced oriented adsorption of antibody fragments for immunosensing platforms[J]. *Biosensors and Bioelectronics*, 2005, 20(11): 2210-2217.

[22] Zhang S, Xia J and Li X. Electrochemical biosensor for detection of adenosine based on structure-switching aptamer and amplification with

reporter probe DNA modified Au nanoparticles[J]. *Analytical chemistry*, 2008, 80(22): 8382-8388.

[23] Ansari A A, Kaushik A, Solanki P and Malhotra B. Sol–gel derived nanoporous cerium oxide film for application to cholesterol biosensor[J]. *Electrochemistry communications*, 2008, 10(9): 1246-1249.

[24] Tang J, Tang D, Su B, Huang J, Qiu B and Chen G. Enzyme-free electrochemical immunoassay with catalytic reduction of p-nitrophenol and recycling of p-aminophenol using gold nanoparticles-coated carbon nanotubes as nanocatalysts[J]. *Biosensors and Bioelectronics*, 2011, 26(7): 3219-3226.

[25] Xiang Y, Zhang Y, Qian X, Chai Y, Wang J and Yuan R. Ultrasensitive aptamer-based protein detection via a dual amplified biocatalytic strategy[J]. *Biosensors and Bioelectronics*, 2010, 25(11): 2539-2542.

[26] Chłopek J, Czajkowska B, Szaraniec B, Frackowiak E, Szostak K and Beguin F. In vitro studies of carbon nanotubes biocompatibility[J]. *Carbon*, 2006, 44(6): 1106-1111.

[27] Lobo A O, Antunes E F, Palma M B, Pacheco-Soares C, Trava-Airoldi V J and Corat E J. Biocompatibility of multi-walled carbon nanotubes grown on titanium and silicon surfaces[J]. *Materials Science and Engineering: C*, 2008, 28(4): 532-538.

[28] Wei Q, Xiang Z, He J, Wang G, Li H, Qian Z and Yang M.

Dumbbell-like Au-Fe_3O_4 nanoparticles as label for the preparation of electrochemical immunosensors[J]. *Biosensors and Bioelectronics*, 2010, 26(2): 627-631.

[29] Wang C, Xu C, Zeng H and Sun S. Recent Progress in Syntheses and Applications of Dumbbell-like Nanoparticles[J]. *Advanced materials*, 2009, 21(30): 3045-3052.

[30] Empedocles S and Bawendi M. Quantum-confined stark effect in single CdSe nanocrystallite quantum dots[J]. *Science*, 1997, 278(5346): 2114-2117.

[31] Wong S S, Woolley A T, Joselevich E, Cheung C L and Lieber C M. Covalently-Functionalized Single-Walled Carbon Nanotube Probe Tips for Chemical Force Microscopy[J]. *Journal of the American Chemical Society*, 1998, 120(33): 8557-8558.

[32] Niu H, Yuan R, Chai Y, Mao L, Liu H and Cao Y. Highly amplified electrochemiluminescence of peroxydisulfate using bienzyme functionalized palladium nanoparticles as labels for ultrasensitive immunoassay[J]. *Biosensors and Bioelectronics*, 2013, 39(1): 296-299.

[33] Han J, Zhuo Y, Chai Y, Yu Y, Liao N and Yuan R. Electrochemical immunoassay for thyroxine detection using cascade catalysis as signal amplified enhancer and multi-functionalized magnetic graphene sphere as signal tag[J]. *Analytica Chimica Acta*, 2013, 790(0): 24-30.

[34] Gao Z-D, Guan F-F, Li C-Y, Liu H-F and Song Y-Y.

Signal-amplified platform for electrochemical immunosensor based on TiO_2 nanotube arrays using a HRP tagged antibody-Au nanoparticles as probe[J]. *Biosensors and Bioelectronics*, 2013, 41: 771-775.

[35] Morales-Cid G, Fekete A, Simonet B M, Lehmann R, Cárdenas S, Zhang X, Valcárcel M and Schmitt-Kopplin P. In situ synthesis of magnetic multiwalled carbon nanotube composites for the clean-up of (fluoro) quinolones from human plasma prior to ultrahigh pressure liquid chromatography analysis[J]. *Analytical chemistry*, 2010, 82(7): 2743-2752.

[36] Frens G. Controlled nucleation for the regulation of the particle size in monodisperse gold suspensions[J]. *Nature*, 1973, 241(105): 20-22.

[37] Singh K V, Pandey R R, Wang X, Lake R, Ozkan C S, Wang K and Ozkan M. Covalent functionalization of single walled carbon nanotubes with peptide nucleic acid: nanocomponents for molecular level electronics[J]. *Carbon*, 2006, 44(9): 1730-1739.

[38] Hong R Y, Pan T T and Li H Z. Microwave synthesis of magnetic Fe_3O_4 nanoparticles used as a precursor of nanocomposites and ferrofluids[J]. *Journal of Magnetism and Magnetic Materials*, 2006, 303(1): 60-68.

[39] Zhang S, Du B, Li H, Xin X, Ma H, Wu D, Yan L and Wei Q. Metal ions-based immunosensor for simultaneous determination of estradiol and diethylstilbestrol[J]. *Biosensors and Bioelectronics*, 2014, 52(0): 225-231.

[40] Zhang Q, Lee I, Ge J, Zaera F and Yin Y. Surface-Protected Etching of Mesoporous Oxide Shells for the Stabilization of Metal Nanocatalysts[J]. *Advanced Functional Materials*, 2010, 20(14): 2201-2214.

[41] Guo A, Li Y, Cao W, Meng X, Wu D, Wei Q and Du B. An electrochemical immunosensor for ultrasensitive detection of carbohydrate antigen 199 based on Au@Cu_xO_S yolk–shell nanostructures with porous shells as labels[J]. *Biosensors and Bioelectronics*, 2015, 63(0): 39-46.